



Cite this: *RSC Adv.*, 2017, 7, 38581

E/Z isomerization effects on aggregation-enhanced emission of tetraphenylethene derivatives assisted by host–guest recognition†

Lijie Li, Lipeng He, Xiaoning Liu, Haomin Liu, Linlin Hu, Pingxia Guo and Weifeng Bu *

Received 9th June 2017
Accepted 29th July 2017

DOI: 10.1039/c7ra06475f

rsc.li/rsc-advances

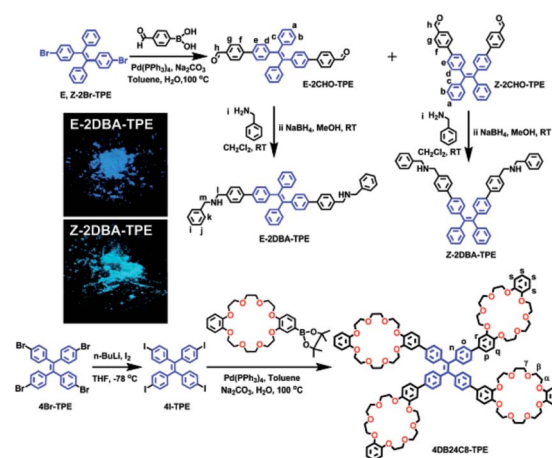
Pure stereoisomers of tetraphenylethene derivatives functionalized with dibenzylamine groups, *E* and *Z* conformers, were successfully synthesized. Their aggregation-enhanced emissions, which occurred through host–guest recognition with a dibenzo-24-crown-8 based tetraphenylethene under an acid condition, showed recognizable isomerization effects.

In nature, there are many fascinating *E* and *Z* conformers, both of which possess unique and elegant properties. *Cis-trans* isomers have the same chemical formula but with different geometrical positions in space, leading to very different functionalities. Therefore, their synthesis and separation are of great importance in medicinal industry,¹ mechanical devices,² and information storage.³ Tetraphenylethene (TPE) is intensively emissive in solid or aggregated states, but not in dilute solution.⁴ This aggregation-induced emission (AIE) active molecule can be easily functionalized at the para position of the phenyl groups and has been utilized as a building block to develop AIE or aggregation-enhanced emission (AEE) materials. However, TPE derivatives are commonly collected as a stereoisomeric mixture containing both *E* and *Z* conformers. This situation does not permit scientists to distinguish the steric effects on the AIE or AEE properties. In only a few case studies,^{1a,c,5} the *E* isomer of TPE derivatives has shown a different AIE behavior from the *Z* isomer. The remaining challenge is how to efficiently separate the pure *E* and *Z* stereoisomers of TPE derivatives.

Recently, Sun's group^{6a} and we^{6b,c} have developed a strategy of host–guest recognition of crown ethers with dibenzylammoniums to activate the AIE or AEE features of TPE derivatives and TPE-containing polymers, leading to remarkable fluorescence enhancements in solution. The reduplicative complexation of the crown ethers with the dibenzylammonium groups controlled by acid–base reactions induces an aggregate transition from micellar to vesicular. In our ongoing study in

this field, the host–guest recognition and AIE features of *E* and *Z* stereoisomers were merged together for the first time. Herein, we report on the design and separation of pure TPE stereoisomers functionalized with two dibenzylamine groups, *E*-2DBA–TPE and *Z*-2DBA–TPE (Scheme 1). When they were titrated with acid in a THF solution of 4DB24C8–TPE that contained four dibenzo-24-crown-8 (DB24C8) rings (Scheme 1), their emission bands showed a blue shift of 67 and 38 nm, respectively, and synchronously the fluorescence intensities increased significantly with a factor of 157 and 97. Here, the *E/Z* isomerization effect can be distinguished clearly.

The synthetic routes of *E*-2DBA–TPE and *Z*-2DBA–TPE were described in Scheme 1. Pure stereoisomers, *E*-2CHO–TPE and *Z*-2CHO–TPE, were successfully separated from the conformer mixtures of formyl functionalized TPE derivatives by the



Scheme 1 Synthetic routes of *E*-2DBA–TPE, *Z*-2DBA–TPE and 4DB24C8–TPE. Inset: photographs of solid powders of *E*-2DBA–TPE and *Z*-2DBA–TPE under UV irradiation at 365 nm.

Key Laboratory of Nonferrous Metals Chemistry and Resources Utilization of Gansu Province, State Key Laboratory of Applied Organic Chemistry, College of Chemistry and Chemical Engineering, Lanzhou University, Lanzhou City, Gansu Province, China. E-mail: buwf@lzu.edu.cn

† Electronic supplementary information (ESI) available: Synthesis and characterization of 4DB24C8–TPE, *E*-2DBA–TPE and *Z*-2DBA–TPE, DLS plots, SEM and TEM images of *E/Z* supramolecular polymers. See DOI: 10.1039/c7ra06475f



macroscopic technique of column chromatography. The treatments of *E*-2CHO-TPE and *Z*-2CHO-TPE with benzylamine *in situ* produced the corresponding imine compounds, which were further reduced with sodium borohydride to afford the target compounds of *E*-2DBA-TPE and *Z*-2DBA-TPE, respectively. 4DB24C8-TPE was synthesized *via* a Suzuki cross-coupling reaction of Bpin-DB24C8 with 4I-TPE (Scheme 1). All of the intermediate compounds and final products were fully characterized by ^1H , ^{13}C NMR (Fig. S1–S28 \dagger), and high-resolution electrospray ionization mass spectra (Fig. S29 \dagger) together with FTIR spectra (Fig. S30 and S31 \dagger). The purity of the samples was further confirmed by melting points and elemental analyses (see the details in the ESI \dagger). The geometry structures of the *E* and *Z* isomers were further confirmed by NOESY and COSY NMR spectroscopy (Fig. S13–S27 \dagger).

The ^1H NMR spectra of *E*-2CHO-TPE and *Z*-2CHO-TPE and their stereoisomer mixture were displayed in Fig. 1a–c. From *E* to *Z* stereoisomer, the resonances for the aromatic protons H_e and H_d showed recognizable downfield shifts of 0.03 and 0.02 ppm, respectively. For the protons H_c , the resonance signal was shifted upfield with 0.05 ppm. Similar resonance shifts were also found in the ^1H NMR spectra of *E*-2DBA-TPE and *Z*-2DBA-TPE (Fig. S28 \dagger). Both *E*-2DBA-TPE and *Z*-2DBA-TPE were further analyzed by using the NOESY and COSY NMR spectra (Fig. S21–S27 \dagger and 1d). For *E*-2DBA-TPE, the resonance at 7.57 corresponded to the aromatic proton H_f . This signal was clearly correlated with the resonances at $\delta = 7.44$ and 7.41 (Fig. S22 and S23 \dagger). This observation allowed us to assign them to the H_e and H_g protons, respectively. Subsequently, the signal correlation of

H_e with the resonance at $\delta = 7.17$ led to the clear attribution of this peak to $\text{H}_{d,d',d'',d'''}$ in A and B phenyl rings. Following these assignments, the proton resonance at 7.12 was due to $\text{H}_{c,c',c'',c'''}$ in the rings of C and D. Accordingly, the resonances at $\delta = 7.16$ –7.12 ppm were assigned to the H_a and H_b protons. As marked by the black arrows in Fig. 1d, the red cross peaks revealed a clear correlation between $\text{H}_{c,c',c'',c'''}$ and $\text{H}_{d,d',d'',d'''}$. However, this correlation was not found in the corresponding COSY NMR spectrum (Fig. S22 and S23 \dagger). This control observation indicated that the rings of B and D were close in space and here on the same side of the central double bond. However, we did not find any correlation between $\text{H}_{c,c',c'',c'''}$ and $\text{H}_{d,d',d'',d'''}$ in *Z*-2DBA-TPE (Fig. S24–S27 \dagger). This was reasonable when one considered that the rings of A and C were far from B and D in the *Z* isomer.

E-2DBA-TPE and *Z*-2DBA-TPE showed typical AIE properties in the solid states (Fig. S32 and Table S1 \dagger) and THF/water mixtures (Fig. S33–S37 \dagger). When the water fraction was 99%, the fluorescence intensities reached their maximum values with enhancement factors of 134 and 163, respectively. Therefore, their AIE can be efficiently distinguished by the degree of fluorescence enhancements in the THF/water mixture (Fig. S34 \dagger). This was consistent with previously reported AIE properties of TPE-based stereoisomers.^{1a,5a} A similar AIE feature was also found in the case of 4DB24C8-TPE (Fig. S34 \dagger) but with a maximum fluorescence enhancement of only 35 at the water fraction of 95%.

When 2.4 equivalents of HPF_6 were added into a mixture of 4DB24C8-TPE and *E*-2DBA-TPE in CD_2Cl_2 , in which the DBA groups were protonated into dibenzylammoniums, significant changes occurred in the ^1H NMR spectra (Fig. 2a and b). All of the proton signals were greatly broadened and complicated. Four new broad bands appeared at $\delta = 4.48$, 4.62, 4.91, and 5.07 ppm (Fig. 2b). According to previously reported ^1H NMR result on host-guest recognition between DB24C8 and dibenzylammonium groups,⁷ these resonances were clearly assigned to the benzylic methylene protons ($\text{H}_{1c} + \text{H}_{mc}$) adjacent to the NH_2^+ centers hosted by the DB24C8 rings. These shifted, broadened, and complicated resonances suggested that a supramolecular hyperbranched polymer (SHP)⁸ formed in solution by the A_4

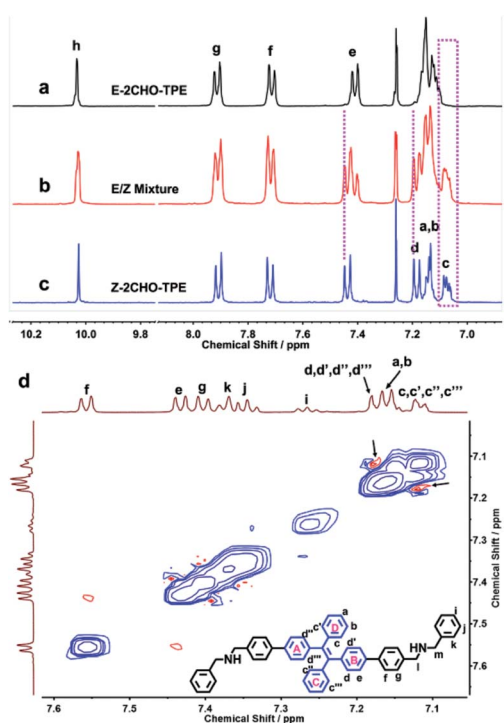


Fig. 1 ^1H NMR spectra (400 MHz, CDCl_3) of *E*-2CHO-TPE (a), *E/Z*-2CHO-TPE stereoisomer mixture (b) and *Z*-2CHO-TPE (c). ^1H NOESY spectrum of *E*-2DBA-TPE (d).

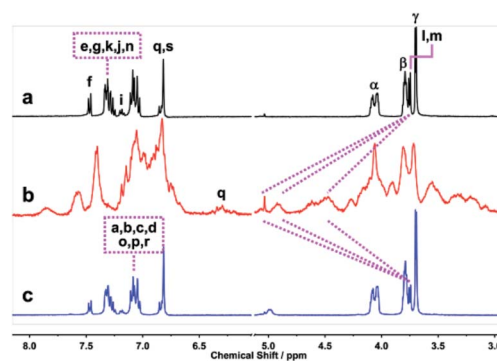


Fig. 2 Partial ^1H NMR spectra (400 MHz, CD_2Cl_2 , (a) of 0.5 mM 4DB24C8-TPE and 1.0 mM *E*-2DBA-TPE, (b) obtained by adding 2.4 equivalents of HPF_6 to the solution of (a), and (c) obtained by adding 2.8 equivalents of P_1 -tBu to the solution of (b).



(4DB24C8-TPE) and B₂ (*E*-2DBA-TPE) monomers through host-guest recognition of the DB24C8 rings with the dialkylammonium ions. With reference to the previous ¹H NMR studies on this class of SHPs,^{7g,k} the isolated and broad signal at 6.30 ppm was due to the complexed aromatic proton H_q. This resonance was independent of those signals for the complexed benzylic methylene protons (H_{lc} + H_{mc}). This situation allowed us to determine the percentage recognition (*p*) and polymerization degree (*n*) according to the following equation: $p = n/(n + 1) = A(H_{lc} + H_{mc})/[4A(H_q)]$, where $A(H_q)$ and $A(H_{lm} + H_{lc})$ are the average integrals of H_q and (H_{lm} + H_{lc}), respectively. Accordingly, the *p* and *n* values were calculated to be 99% and 99 at a DB24C8 concentration of 2.0×10^{-3} mol L⁻¹, respectively. This permitted the calculation of the molecular weight (*M_s*) to be 4.5×10^5 g mol⁻¹. The subsequent addition of 2.8 equivalents of *N*-*tert*-butyl-*N',N',N'',N''',N''''*-hexamethylphosphorimidic triamide (P₁-*t*Bu), a strong base in the same solution caused a fully recovered ¹H NMR spectrum (Fig. 2c), indicating that the SHP formed reversibly in solution. A similar acid-base controlled SHP was also fabricated by mixing 4DB24C8-TPE and *Z*-2DBA-TPE in CD₂Cl₂ (Fig. S38†). The calculated values of *p*, *n*, and *M_s* were 95%, 19 and 7.9×10^4 g mol⁻¹, much smaller than those in the case of *E*-2DBA-TPE, respectively. This result suggested that the protonated *E*-2DBA-TPE was more easily and fully connected with 4DB24C8-TPE than the protonated *Z*-2DBA-TPE through the host-guest recognition, consistent with the different geometries of the stereoisomers. This reversible supramolecular polymerization was further supported by the DOSY NMR experiments (Fig. S40 and S41†).

With these results in mind, we continued to investigate acid-base controlled AEE features and aggregate morphologies in

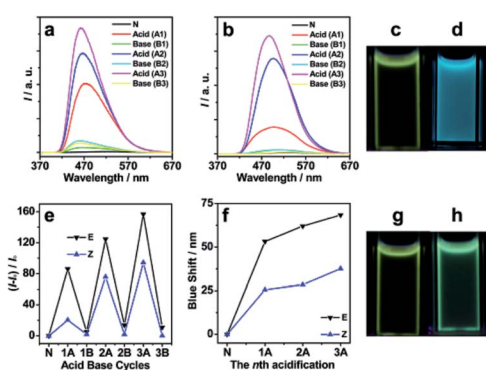


Fig. 3 Fluorescence spectra of the solutions of *E*-2DBA-TPE (a) and (b) *Z*-2DBA-TPE mixed with 4DB24C8-TPE, respectively, under three acid-base reaction cycles. (e) The plots of fluorescence intensities and (f) the blue shifts of *E*-2DBA-TPE and *Z*-2DBA-TPE in the THF solutions upon successive treatments with HCl and NaOH. As revealed by the photographs under UV irradiation at 365 nm, the solutions of *E*-2DBA-TPE (d) and *Z*-2DBA-TPE (h) mixed with 4DB24C8-TPE showed remarkable fluorescence enhancements and impressive blue shifts upon the third acid treatment compared to their respective original solutions (c and g). The concentrations of *E/Z*-2DBA-TPE and 4DB24C8-TPE were controlled at 1.0 and 0.5 mM, respectively. Here, N, A and B denote the neutral solution and its acid and base treatments, respectively. 1, 2 and 3 denote the sequence of the acid-base cycle.

solution. Alternating treatments of the THF mixture solution of 4DB24C8-TPE and *E*-2DBA-TPE or *Z*-2DBA-TPE with HCl and NaOH resulted in consecutive fluorescence enhancement and attenuation (Fig. 3). In the case of *E*-2DBA-TPE, the fluorescence intensities increased with a factor of 86, 125 and 157 at the first, second, and third acidification, respectively. In contrast, the fluorescence of *Z*-2DBA-TPE was enhanced only to 21, 78, and 97 folds. Both of them showed a stepwise increase in the fluorescence intensities with the acid treatments. With the corresponding base treatments, however, the enhanced fluorescence almost returned back to the original levels. Concomitant with these fluorescence enhancements, the emissive bands were blue-shifted from 530 to 477 (53), 468 (62) and 463 nm (67 nm) for *E*-2DBA-TPE, while the blue shifts of 26, 28 and 38 nm were clearly observed in the case of *Z*-2DBA-TPE. The blue shifts were stepwise amplified with the acid treatments, consistent with the increasing trend of the fluorescence intensities as described above. Such big blue shifts could be clearly seen under UV irradiation at 365 nm by naked eyes, where the emission color changed from yellowish green to blue in the case of *E*-2DBA-TPE (Fig. 3c and d), while for *Z*-2DBA-TPE only to light green (Fig. 3g and h). As addressed previously,^{6b,c} the present stepwise emission enhancements and blue shifts could be due to a synergistic interaction of the host-guest recognition of DB24C8 and dibenzylammonium moieties together with the salting-out effect (Fig. S35†). The latter was originated from the acid-base reaction of NaOH with the dibenzylammonium chloride group to generate NaCl. Here, the impressive blue shifts synchronized with remarkable fluorescence enhancements, which were seldom caught in other supramolecular polymer systems involving AEE effects. The degrees of fluorescence enhancements and blue shifts in the case of *E*-2DBA-TPE were much larger than those in the case of *Z*-2DBA-TPE. This observation was in excellent agreement with much easier supramolecular polymerization of the protonated *E*-2DBA-TPE with 4DB24C8-TPE than the protonated *Z*-2DBA-TPE as stated above.

To understand the observed photophysical phenomena, the above solutions were subjected to dynamic light scattering (DLS) and transmission electron microscopy (TEM) measurements. The DLS plot of the initial mixture solution of *E*-2DBA-TPE or *Z*-2DBA-TPE with 4DB24C8-TPE offered a hydrodynamic diameter (*D_h*) of 1.8 nm (Fig. 4a). This value was consistent with the molecular sizes of those TPE derivatives. Upon three-cycle acid treatments with HCl, the value of *D_h* increased to 563, 2485, and 6014 nm for *E*-2DBA-TPE, respectively, while in the case of *Z*-2DBA-TPE, the *D_h* value was 157, 1838, and 2431 nm. The stepwise increasing *D_h* values coincided with the increasing trends of the fluorescence enhancements and blue shifts with the acidification cycles as addressed above. Therefore, these aggregates suppressed the intramolecular rotation of phenyl groups in both *E/Z*-2DBA-TPE and 4DB24C8-TPE in solution, leading to stepwise fluorescence enhancements and blue shifts (Fig. 3). In total, the sizes of the aggregates formed by the protonated *E*-2DBA-TPE with 4DB24C8-TPE were much bigger than those by the protonated *Z*-2DBA-TPE with 4DB24C8-TPE. These DLS data were in line with the aforementioned ¹H NMR, AEE, and blue shift results. TEM images showed that the SHP



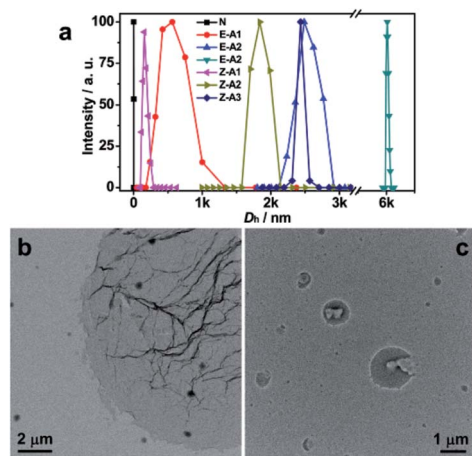


Fig. 4 DLS plots of *E*-2DBA-TPE and *Z*-2DBA-TPE mixed with 4DB24C8-TPE in THF under acid conditions (a). TEM images of *E*-2DBA-TPE (b) and *Z*-2DBA-TPE (c) mixed with 4DB24C8-TPE under the third acidification. The concentrations of *E*- or *Z*-2DBA-TPE and 4DB24C8-TPE were controlled at 1.0 and 0.5 mM, respectively. Here, N, A denote the neutral solution and its acid and base treatments, respectively. 1, 2 and 3 denote the sequence of the acid–base cycle.

fabricated by the protonated *E*-2DBA-TPE and 4DB24C8-TPE self-assembled into sheet like aggregates, while in the case of *Z*-2DBA-TPE, ruptured spheres formed. The more ordered forms of TPE derivatives in the nanosheets explained well the much larger blue shifts and fluorescence enhancements in the case of *E*-2DBA-TPE. All of these distinct behaviors stemmed from the *E/Z* isomerization effect of the stereoisomers, *E*-2DBA-TPE and *Z*-2DBA-TPE during the host–guest recognition process under acid conditions.

In summary, we have isolated and characterized TPE-based stereoisomers, *E*-2DBA-TPE and *Z*-2DBA-TPE. Upon consecutive treatments with acid and base, they can be reversibly copolymerized with 4DB24C8-TPE into SHPs through host–guest recognition, leading to reversible fluorescence enhancements and blue shifts. However, both the supramolecular polymerization and corresponding photophysical changes were more significant in the case of *E*-2DBA-TPE than in *Z*-2DBA-TPE. This difference is originated from their different geometries leading to distinguishable percentage recognitions and polymerization degrees. The present supramolecular system on the basis of TPE stereoisomers displays tunable photophysical properties and morphological features and are of great importance to potential applications in the fields of chemical and biological sensors and optoelectronics.

Acknowledgements

This work is supported by the NSFC (21474044 and 21674044), the Fundamental Research Funds for the Central Universities (lzujbky-2015-k04 and lzujbky-2016-42) and the Open Project of State Key Laboratory of Supramolecular Structure and Materials of Jilin University (sklssm201701). The project was supported by Open Research Fund of State Key Laboratory of Polymer Physics and Chemistry, Changchun Institute of Applied Chemistry, Chinese Academy of Sciences (201626).

Notes and references

- (a) X. Fang, Y. Zhang, K. Chang, Z. Liu, X. Su, H. Chen, S. X. Zhang, Y. Liu and C. Wu, *Chem. Mater.*, 2016, **28**, 6628; (b) Y. Yuan, C. Zhang and B. Liu, *Chem. Commun.*, 2015, **51**, 8626; (c) M. Zhang, X. Yin, T. Tian, Y. Liang, W. Li, Y. Lan, J. Li, M. Zhou, Y. Ju and G. Li, *Chem. Commun.*, 2015, **51**, 10210.
- (a) D. Dijken, P. Kovaříček, S. P. Ihrig and S. Hecht, *J. Am. Chem. Soc.*, 2015, **137**, 14982; (b) Y. Liu, T. Shan, L. Yao, Q. Bai, Y. Guo, J. Li, X. Han, W. Li, Z. Wang, B. Yang, P. Lu and Y. Ma, *Org. Lett.*, 2015, **17**, 6138; (c) S. Guo, K. Matsukawa, T. Miyata, T. Okubo, K. Kuroda and A. Shimojima, *J. Am. Chem. Soc.*, 2015, **137**, 15434.
- (a) V. Serreli, C. Lee, E. Kay and D. Leigh, *Nature*, 2007, **445**, 523; (b) J. W. Chung, S.-J. Yoon, B.-K. An and S. Y. Park, *J. Phys. Chem. C*, 2013, **117**, 11285.
- (a) J. Luo, Z. Xie, J. W. Y. Lam, L. Cheng, H. Chen, C. Qiu, H. S. Kwok, X. Zhan, Y. Liu, D. Zhu and B. Z. Tang, *Chem. Commun.*, 2001, 1740; (b) B.-K. An, S.-K. Kwon, S.-D. Jung and S. Y. Park, *J. Am. Chem. Soc.*, 2002, **124**, 14410; (c) L. Liu, G. Zhang, J. Xiang, D. Zhang and D. Zhu, *Org. Lett.*, 2008, **10**, 4581; (d) J. He, B. Xu, F. Chen, H. Xia, K. Li, L. Ye and W. Tian, *J. Phys. Chem. C*, 2009, **113**, 9892; (e) Q. Chen, N. Bian, C. Cao, X.-L. Qiu, A.-D. Qi and B.-H. Han, *Chem. Commun.*, 2010, **46**, 4067; (f) H. Lu, B. Xu, Y. Dong, F. Chen, Y. Li, Z. Li, J. He, H. Li and W. Tian, *Langmuir*, 2010, **26**, 6838; (g) Y. Hong, J. W. Y. Lam and B. Z. Tang, *Chem. Soc. Rev.*, 2011, **40**, 5361; (h) R. Hu, J. L. Maldonado, M. Rodriguez, C. Deng, C. K. W. Jim, J. W. Y. Lam, M. M. F. Yuen, G. Ramos-Ortiz and B. Z. Tang, *J. Mater. Chem.*, 2012, **22**, 232; (i) W. Wu, S. Ye, L. Huang, L. Xiao, Y. Fu, Q. Huang, G. Yu, Y. Liu, J. Qin, Q. Lia and Z. Li, *J. Mater. Chem.*, 2012, **22**, 6374; (j) X. Wang, J. Hu, T. Liu, G. Zhang and S. Liu, *J. Mater. Chem.*, 2012, **22**, 8622; (k) Z. Wang, S. Chen, J. W. Y. Lam, W. Qin, R. T. K. Kwok, N. Xie, Q. Hu and B. Z. Tang, *J. Am. Chem. Soc.*, 2013, **135**, 8238; (l) Z. Wang, B. Xu, L. Zhang, J. Zhang, T. Ma, J. Zhang, X. Fu and W. Tian, *Nanoscale*, 2013, **5**, 2065; (m) R. Yoshii, A. Hirose, K. Tanaka and Y. Chujo, *J. Am. Chem. Soc.*, 2014, **136**, 18131; (n) R. Hu, N. L. C. Leung and B. Z. Tang, *Chem. Soc. Rev.*, 2014, **43**, 4494; (o) J. Mei, N. L. C. Leung, R. T. K. Kwok, J. W. Y. Lam and B. Z. Tang, *Chem. Rev.*, 2015, **115**, 11718; (p) G. Liang, J. Wu, H. Gao, Q. Wu, J. Lu, F. Zhu and B. Z. Tang, *ACS Macro Lett.*, 2016, **5**, 909; (q) X. You, H. Ma, Y. Wang, G. Zhang, Q. Peng, L. Liu, S. Wang and D. Zhang, *Chem.-Asian J.*, 2017, **12**, 1013; (r) L. Zhu, R. Wang, L. Tan, X. Liang, C. Zhong and F. Wu, *Chem.-Asian J.*, 2016, **11**, 2932; (s) J. Tong, Y. Wang, J. Mei, J. Wang, A. Qin, J. Z. Sun and B. Z. Tang, *Chem.-Eur. J.*, 2014, **20**, 4661.
- (a) J. Wang, J. Mei, R. Hu, J. Sun, A. Qin and B. Tang, *J. Am. Chem. Soc.*, 2012, **134**, 9956; (b) C.-J. Zhang, G. Feng, S. Xu, Z. Zhu, X. Lu, J. Wu and B. Liu, *Angew. Chem., Int. Ed.*, 2016, **55**, 1.



- 6 (a) W. Bai, Z. Wang, J. Tong, J. Mei, A. Qin, J. Z. Sun and B. Z. Tang, *Chem. Commun.*, 2015, **51**, 1089; (b) L. He, X. Liu, J. Liang, Y. Cong, Z. Weng and W. Bu, *Chem. Commun.*, 2015, **51**, 7148; (c) L. He, L. Li, X. Liu, J. Wang, H. Huang and W. Bu, *Polym. Chem.*, 2016, **7**, 3722.
- 7 (a) P. R. Ashton, P. J. Campbell, E. J. T. Chrystal, P. T. Glink, S. Menzer, D. Philp, N. Spencer, J. F. Stoddart, P. A. Tasker and D. J. Williams, *Angew. Chem., Int. Ed. Engl.*, 1995, **34**, 1865; (b) S. J. Cantrill, G. J. Youn and J. F. Stoddart, *J. Org. Chem.*, 2001, **66**, 6857; (c) H. W. Gibson, N. Yamaguchi and J. W. Jones, *J. Am. Chem. Soc.*, 2003, **125**, 3522; (d) F. Wang, C. Han, C. He, Q. Zhou, J. Zhang, C. Wang, N. Li and F. Huang, *J. Am. Chem. Soc.*, 2008, **130**, 11254; (e) Y.-S. Su, J.-W. Liu, Y. Jiang and C.-F. Chen, *Chem.–Eur. J.*, 2011, **17**, 2435; (f) B. Yu, B. Wang, S. Guo, Q. Zhang, X. Zheng, H. Lei, W. Liu, W. Bu, Y. Zhang and X. Chen, *Chem.–Eur. J.*, 2013, **19**, 4922; (g) B. Yu, S. Guo, L. He and W. Bu, *Chem. Commun.*, 2013, **49**, 3333; (h) H. Li, X. Fan, W. Tian, H. Zhang, W. Zhang and Z. Yang, *Chem. Commun.*, 2014, **50**, 14666; (i) S. Guo, J. Zhang, B. Wang, Y. Cong, X. Chen and W. Bu, *RSC Adv.*, 2014, **4**, 51754; (j) L. He, J. Liang, Y. Cong, X. Chen and W. Bu, *Chem. Commun.*, 2014, **50**, 10841; (k) L. Li, X. Zheng, B. Yu, L. He, J. Zhang, H. Liu, Y. Cong and W. Bu, *Polym. Chem.*, 2016, **7**, 287.
- 8 W. Tian, X. Li and J. Wang, *Chem. Commun.*, 2017, **53**, 2531.

